JOURNAL OF MATERIALS SCIENCE 19 (1984) 2731–2748

SiC filament/titanium matrix composites regarded as model composites

Part 1 *Filament microanalysis and strength characterization*

P. MARTINEAU, M. LAHAYE, R. PAILLER, R. NASLAIN
Laboratoire de Chimie du Solide du CNRS, Université de Bordeaux-I 351, Cours de la Libération, 33405 Talence, France

M. COUZI, F. CRUEGE
Laboratoire de Spectroscopie Infrarouge associé au CNRS, LA 124, Université de Bordeaux-I, 351, Cours de la Libération, 33405 Talence, France

Two types of large diameter SiC CVD filaments have been investigated on both chemical and mechanical standpoints: a 100 μm filament with a tungsten core (from SNPE) and three 140 μm filaments with carbon cores and surface coatings (from AVCO). On the basis of microprobe (X-ray, Auger and Raman), X-ray diffraction and SEM analyses, it appears that the former is made of a single homogeneous stoichiometric SiC deposit while the latter are mainly made of two concentric shells (the inner being a SiC+C mixture and the outer almost pure SiC). All the C-core filaments had received a surface coating (either pure pyrocarbon or SiC+C mixture) presumably to protect the brittle SiC deposit against abrasion due to handling in opposition to the W-core filament which seems to have no surface coating at all. The W-core filament, although smaller in diameter, is weaker than the C-core filaments (average UTS of 3 and 4 GPa respectively for a 40 mm gauge length). However, its strength distribution is much narrower (Weibull moduli of 7–8 and 2–5 respectively). Failures of most filaments appear to have a multimodal character.

1. Introduction

The mechanical properties of metal matrix composites are closely related to the fibre–matrix (FM) interfacial phenomena occurring at high (or even medium) temperatures during their synthesis or utilization. This is mainly due to the fact that brittle fibres (e.g. carbon, silicon carbide, boron nitride and to a lesser extent alumina) or filaments (coated or uncoated boron, silicon carbide) used for the reinforcement of metals are generally very reactive. As a result, when such fibres or filaments are heated within a metal matrix, chemical reactions, mainly controlled by diffusion, take place at each fibre–matrix interface, giving rise to a FM reaction zone, usually brittle, whose thickness increases against time at a given temperature. When the FM reaction is very limited (reaction zone of the order of a few thousands of nanometres), it may have a beneficial effect since it results in strong interfaces and good adhesion allowing an efficient load transfer from matrix to fibres. On the contrary, when the FM reaction becomes too important, it may generate a new population of stress concentrators at the brittle fibre surface with a strong weakening of the reinforcing fibrous material. Therefore, the knowledge of the FM interfacial chemistry is a necessary and fundamental step in the development of any metal–matrix composite. This had been already well illustrated in the case of boron–titanium composites [1–5].

One of the main drawbacks of boron filaments lies in the fact that their strength significantly decreases with increasing temperature. Further-

0022–2461/84 $03.00 + .12

more, boron reacts very rapidly with most light metals used as matrices. Silicon carbide, either as tows of small diameter fibres or large size monofilaments, appears to be a more suitable material for the reinforcement of metals. It has a higher melting point and a much better chemical inertia towards chemical reactants (including air and metals). SiC fibres or filaments are characterized by high strength and stiffness and keep a high fraction of their room temperature mechanical performances over a wide range of temperature [6–11].

Titanium matrix composites up to now were of limited practical interest. Nevertheless, they could be used in the future as structural materials for medium temperature applications. On the other hand, they can be regarded as very convenient model composites, from a fundamental point of view and as far as interfacial FM chemistry is concerned. Titanium has a high melting point (θ_F = 1668° C, with respect to 650° C for magnesium and 660° C for aluminium), a property which makes possible diffusion experiments in a wide range of temperature. It reacts at medium temperature with carbon or silicon and the corresponding binary or ternary phase diagrams are known [12]. Finally, titanium matrix composites can be rather easily prepared by hot pressing [13].

For these reasons, a long term research programme was started several years ago in one of the laboratories of the authors (LCS) to illustrate, from the solid-state chemistry point of view, the relationships that exist between FM interfacial chemistry and mechanical behaviour, in metal–matrix composites [13–15]. It is also thought that the results of this research will help to better the understanding of the behaviour or the related materials of much more practical interest. The present work deals with the microanalysis and strength characterization of large diameter silicon carbide based CVD-filaments.

2. The silicon carbide CVD-filaments

SiC-based filaments of large diameter (100 to 150 μm) are obtained by CVD, on a wire substrate (tungsten or carbon) heated at 1200 to 1400° C, from different gas mixtures whose main components are: a chlorosilane (e.g. CH_3SiCl_3, $(CH_3)_2SiCl_2$ or CH_3SiHCl_2), hydrogen and eventually an alkane (e.g. CH_4 or better C_3H_8 or C_4H_{10}) and/or argon, as schematically shown in Fig. 1 [6–9, 16–18].

The CVD-process does have a few important

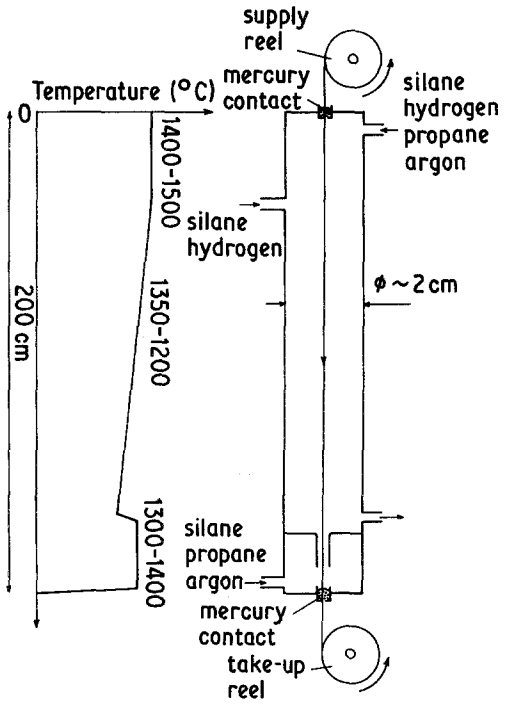

Figure 1 Schematic diagram of a reactor used to produce SiC based filament, after [17].

drawbacks which have been already analysed elsewhere. Its main advantage lies in the fact that it can be used to obtain in one single operation filaments with an optimized composition profile from the core to the external surface resulting in much higher strength and stiffness than those reported, up to now, for the fibres of small diameter obtained by spinning and pyrolysis of a liquid organosilane precursor. Strength and Young's modulus, respectively, as high as 4000 MPa and 420 GPa are currently achieved for the 140 μm CVD carbon core filaments as compared to only 2500 MPa and 180 GPa for the 10 to 20 μm fibres derived from polycarbosilane liquid precursors. Moreover, surface coatings can be easily applied on filaments at the end of the CVD-process, in order to promote wetting by liquid metal matrices and/or to decrease their chemical reactivity with metals. Therefore, SiC-CVD filaments do appear as very high performance fibrous materials for the reinforcement of metals.

The CVD of SiC-based materials from chlorosilanes has been recently the subject of several thermodynamic and experimental studies. Christin *et al.* [19, 20] have shown, from thermodynamic calculations, that the nature of the deposit which is formed at equilibrium from CH_3SiCl_3(MTS)–

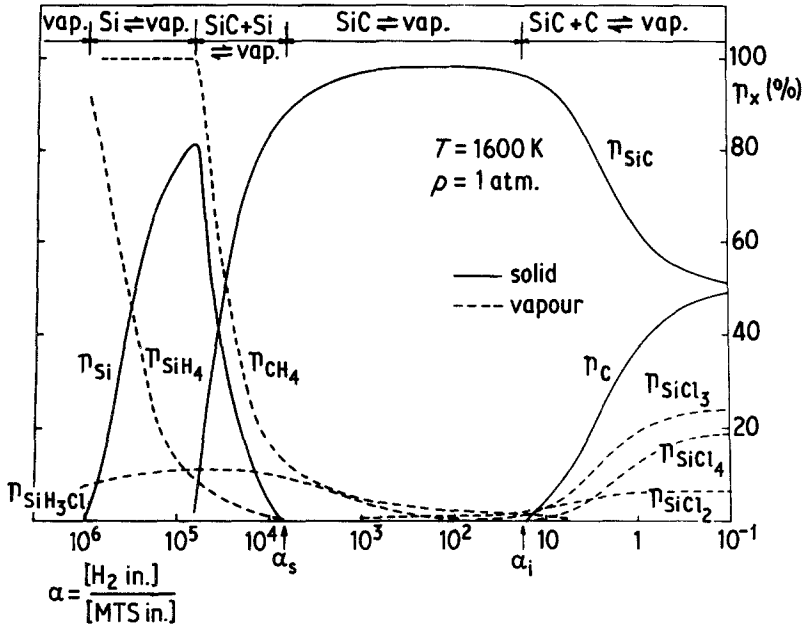

Figure 2 CVD from CH_3SiCl_3 (MTS)–H_2 gas mixtures: thermodynamic yields η_{SiC}, η_C, η_{Si} as a function of $\alpha = [H_{2\,in.}]/[MTS_{in.}]$ at 1600 K and 1 atm, according to Christin *et al.* [19].

H_2 gas mixtures, depends on the initial $\alpha = [H_{2\,in.}]/[MTS_{in.}]$ ratio, at a given temperature and total pressure. The deposit is made of pure SiC for $\alpha_i < \alpha < \alpha_s$ (with $\alpha_i \simeq 14$, $\alpha_s \simeq 8000$ at 1600 K and 1 atm) and of a mixture of SiC and elemental carbon for $\alpha < \alpha_i$. Gas mixtures very rich in hydrogen ($\alpha > \alpha_s$) lead to SiC+Si and even to pure silicon deposits (Fig. 2). Increasing the deposition temperature does not change significantly the α_i value, but strongly modifies the η_{SiC} and η_C thermodynamic yields (Fig. 3). When hydrogen is partly replaced by argon, SiC+C deposits are obtained in a larger composition range (Fig. 4) and finally when the gas mixture no longer contains free hydrogen (i.e. in the case of MTS–argon mixtures), the deposit is a mixture of silicon carbide and elemental carbon, whatever the $\alpha' = [Ar_{in.}]/[MTS_{in.}]$ ratio (Fig. 5) [20, 21]. In the same manner, replacing CH_3SiCl_3 by $(CH_3)_2SiCl_2$ (DDS) (i.e. increasing the C/Si ratio) in the gas mixture increases α_i and adding $SiCl_4$ to CH_3SiCl_3 (i.e. decreasing C/Si) has a reverse effect (Fig. 6). Thus, two important conclusions are drawn from the thermodynamic calculations:

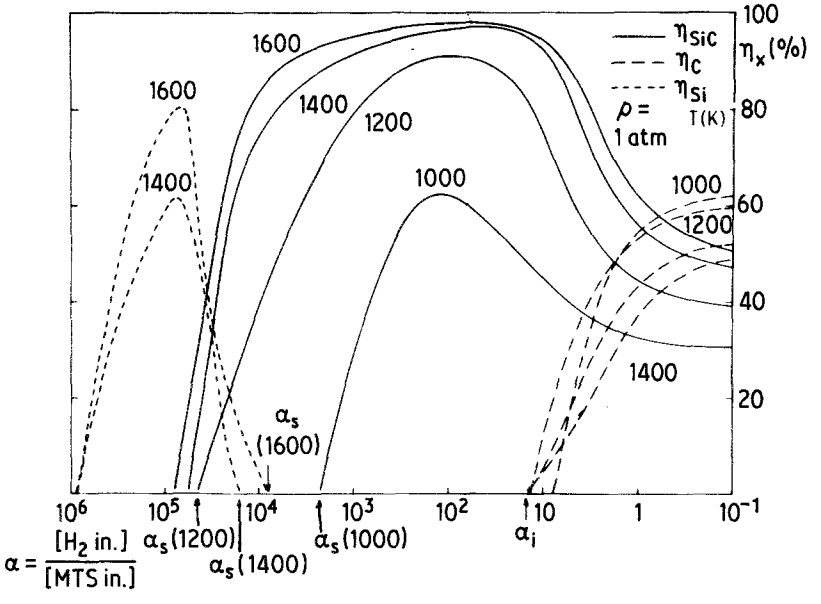

Figure 3 CVD from CH_3SiCl_3 (MTS)–H_2 gas mixtures: thermodynamic yields η_{SiC}, η_C and η_{Si} against α at different temperatures, according to Christin *et al.* [19].

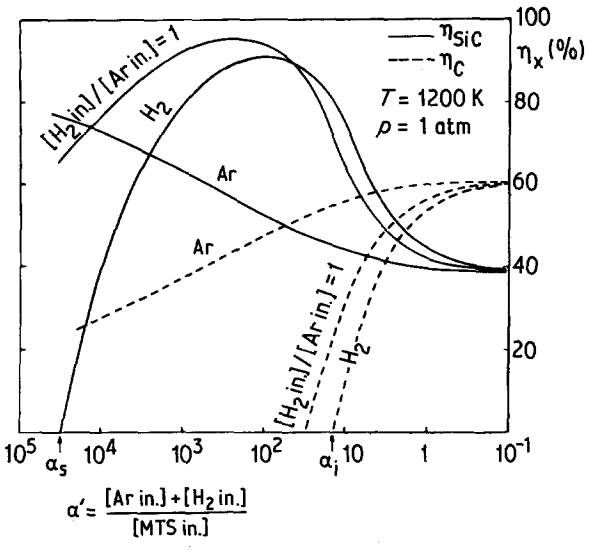

Figure 4 CVD from CH_3SiCl_3 (MTS)–H_2–Ar gas mixtures: thermodynamic yields η_{SiC} and η_C against $\alpha' = ([Ar_{in.}] + [H_{2\ in.}]/[MTS_{in.}]$, according to Christin *et al.* [19].

(i) pure SiC deposition requires addition of rather large amounts of hydrogen to chlorosilanes,

(ii) SiC+C deposits are obtained from hydrogen poor chlorosilane–hydrogen mixtures or better still from chlorosilane–argon mixtures, since in this latter case elemental carbon remains present in the deposit whatever the argon/chlorosilane ratio [20, 21].

Various experimental studies have confirmed the main conclusions of the above thermodynamic approach and particularly the occurrence of elemental carbon in SiC-deposits as well as the important role played by hydrogen added to chlorosilanes [23–32].

Four samples of SiC-CVD filaments have been analysed and used for the synthesis of SiC/Ti composites. All of them are experimental products. One of them, referred to as SiC(3), is a filament, 100 μm in diameter and with a tungsten core, developed a few years ago by SNPE (Paris). The others, from AVCO (Lowell, Mass.), referred to as SiC(1), SiC(2) or SiC(4) are more recent materials but are different, in microstructure, from the SCS-filament presently produced on an industrial level. They are 140 μm in diameter and have a carbon core.

3. X-ray electron probe microanalysis

Silicon X-ray profiles (Si$K\alpha$) were recorded, along a diameter, on polished sections of the filaments. In order to avoid edge effects during polishing, the brittle filaments were embedded in a titanium matrix (i.e. the analysis was performed on polished sections of as-prepared SiC/Ti composites).

The profiles are shown in Fig. 7. It clearly appears that filament SiC(3) has a homogeneous composition from the tungsten core to the external surface, whereas the others exhibit two plateaus of constant silicon concentration. The first plateau (I), near the carbon core, has an average thickness of about 20 μm and the second one (II), on the outside, a thickness ranging from 25 to 32 μm.

A quantitative analysis for silicon, using a SiC single crystal as a standard, was performed on each plateau. Assuming that only silicon and carbon atoms are present and that silicon carbide is

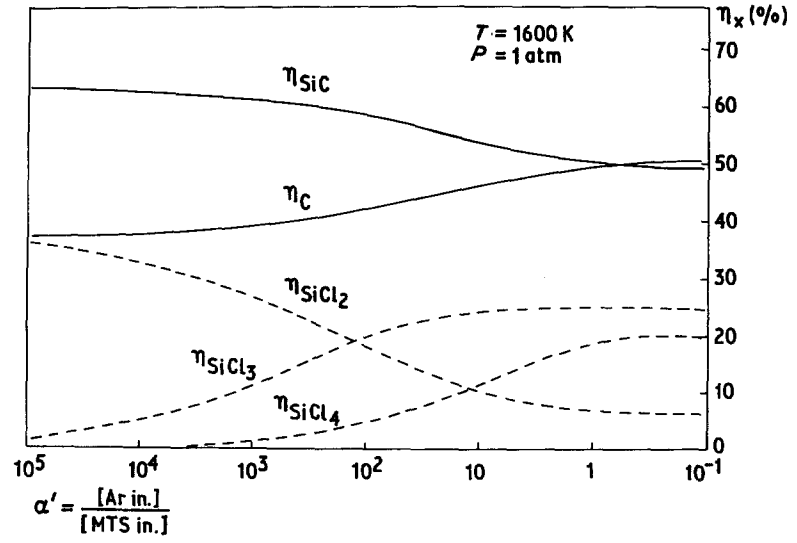

Figure 5 CVD from CH_3SiCl_3 (MTS)–Ar gas mixtures: thermodynamic yields η_{SiC} and η_C against $\alpha' = [Ar_{in.}]/[MTS_{in.}]$, according to Christin [20].

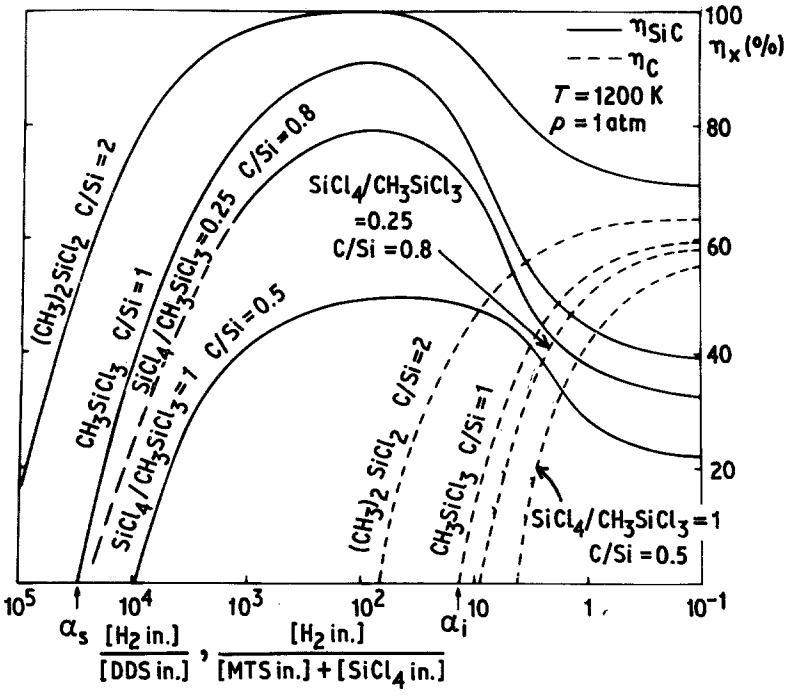

Figure 6 CVD from chlorosilanes–H_2 gas mixtures: thermodynamic yields η_{SiC} and η_C against α, according to Christin *et al.* [19].

stoichiometric, the results are expressed, in Table I, as SiC and free carbon weight percentages.

SiC(3) filament is found to be made of pure stoichiometric SiC from the core to the edge. On the contrary, the other filaments are made of a layer of SiC+C mixture near the carbon core (the percentage of free carbon ranging from about 5 to 10%) surrounded by a deposit of almost pure SiC (except for the SiC(2) filament where a small amount of free carbon is also present).

4. Auger electron probe analysis

Two types of Auger electron microanalysis have been performed with an AES microanalyser characterized by an electron probe diameter of about 200 nm: (i) radial profiles for silicon (Si_{LMM}) and carbon (C_{KLL}) on the polished sections used previously for the X-ray electron probe microanalysis and (ii) depth profiles (carbon, silicon and oxygen (O_{KLL})), by ion sputtering, from the surfaces of the as received filaments.

The radial silicon and carbon profiles recorded on polished sections of the filaments are shown in Fig. 8. They confirm the results of the X-ray microprobe analysis, i.e. the occurrence of two plateaus of different compositions for the carbon core filaments (the inner shell (I) being carbon-rich) and the homogeneous composition of the SiC-deposit in the case of the tungsten core filament.

The depth profile analysis was performed near the external surface of the as-received filaments, in order to establish whether the filaments had been surface treated. Sputtering was achieved with 4.5 keV argon ions, at a rate of about 70 nm min^{-1}

TABLE I Chemical composition of SiC based filaments derived from X-ray electron microprobe analysis for silicon (SiC single crystal standard)

Filaments	Plateau I		Plateau II	
	width (μm)	composition*	width (μm)	composition
SiC(1)	20	SiC 94% C 6%	30	SiC
SiC(2)	20	SiC 90% C 10%	24	SiC 95% C 5%
SiC(3)	45	SiC	–	–
SiC(4)	23	SiC 94% C 6%	27	SiC

*wt %.

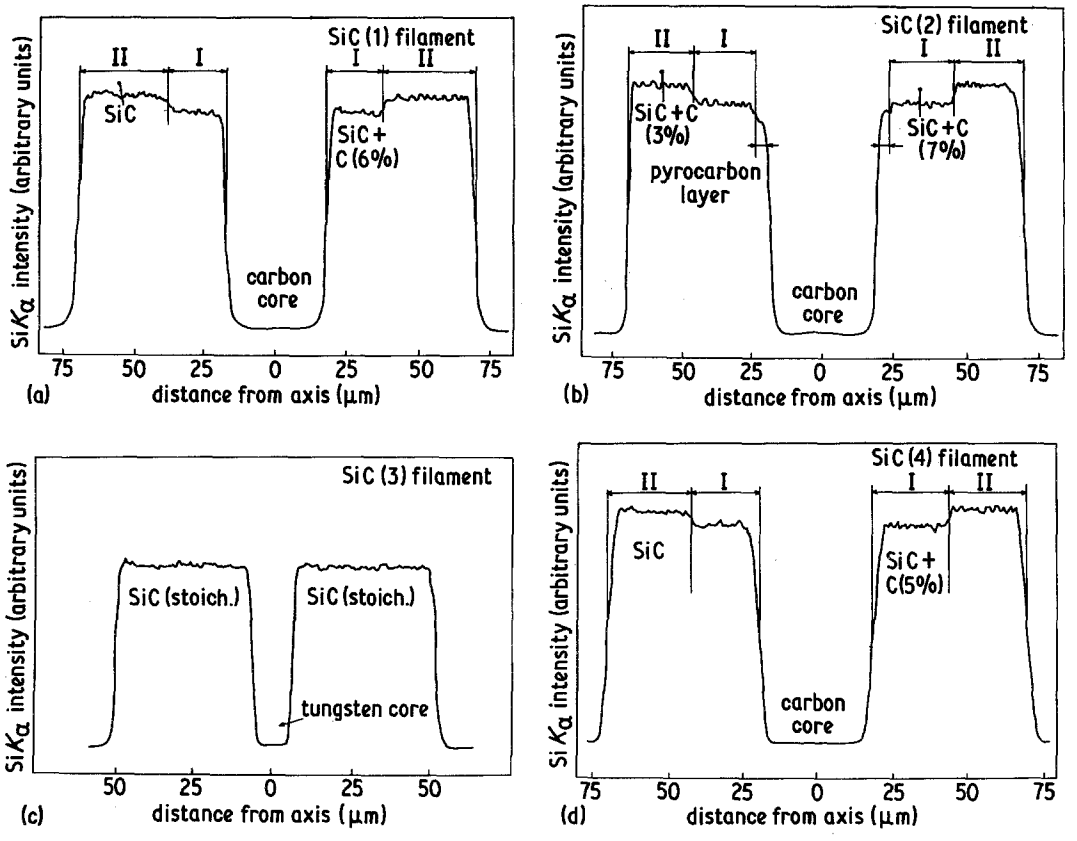

Figure 7 X-ray microprobe radial profiles for silicon (Si$K\alpha$) on polished sections of SiC based CVD-filaments.

(referring to tantalum oxide Ta_2O_5 as a standard) except in the case of the SiC(3) filament where the sputtering rate was first 2.5 nm min^{-1} and then 25 nm min^{-1}. The profiles are shown in Fig. 9.

In each case no significant amount of oxygen was found near the surface of the filaments (see the case of SiC(3)). In the same manner, it seems that the tungsten core stoichiometric SiC filament did not receive any significant surface treatment. On the contrary, all the carbon core AVCO filaments have a surface which is strongly enriched in carbon, the thickness of the carbon-rich layer being wide for filaments SiC(1) and SiC(2) and small for filament SiC(4). Although no accurate sputtering rate calibration was carried out, the respective thicknesses could be of the order of 3.5 to 4 μm for SiC(1) and SiC(2) and of the order of 1 μm for SiC(4).

Furthermore, the variations of the carbon and silicon atomic concentrations within the carbon-rich coating are different. For both SiC(1) and SiC(4), there is a progressive variation in both carbon and silicon concentrations from plateau II (SiC, almost pure) to the external surface of the filament which appears to be almost pure carbon. On the other hand, for SiC(2), the silicon concentration falls very rapidly from 50 at % (inner zone of almost pure SiC) to a very low value (less than 10 at %) within about 1 μm and then remains almost constant up to the neighbourhood of the external surface of the filament where it may slightly re-increase. Therefore, the SiC(2) filament seems to have received a coating essentially made of pure carbon, whereas filaments SiC(1) and SiC(4) are characterized by a smooth transition from almost stoichiometric SiC (plateau II) to a mixture of SiC+C very rich in carbon if not to pure carbon.

5. X-ray diffraction study

The Debye–Scherrer patterns of the as-received filaments shows that all of them are essentially made of the low temperature β-form of silicon carbide (cubic lattice, $T_D2 - F\bar{4}3m$) (Table II). However, a few lines corresponding to a α-hexagonal form are also observed (SiC(1); SiC(3)

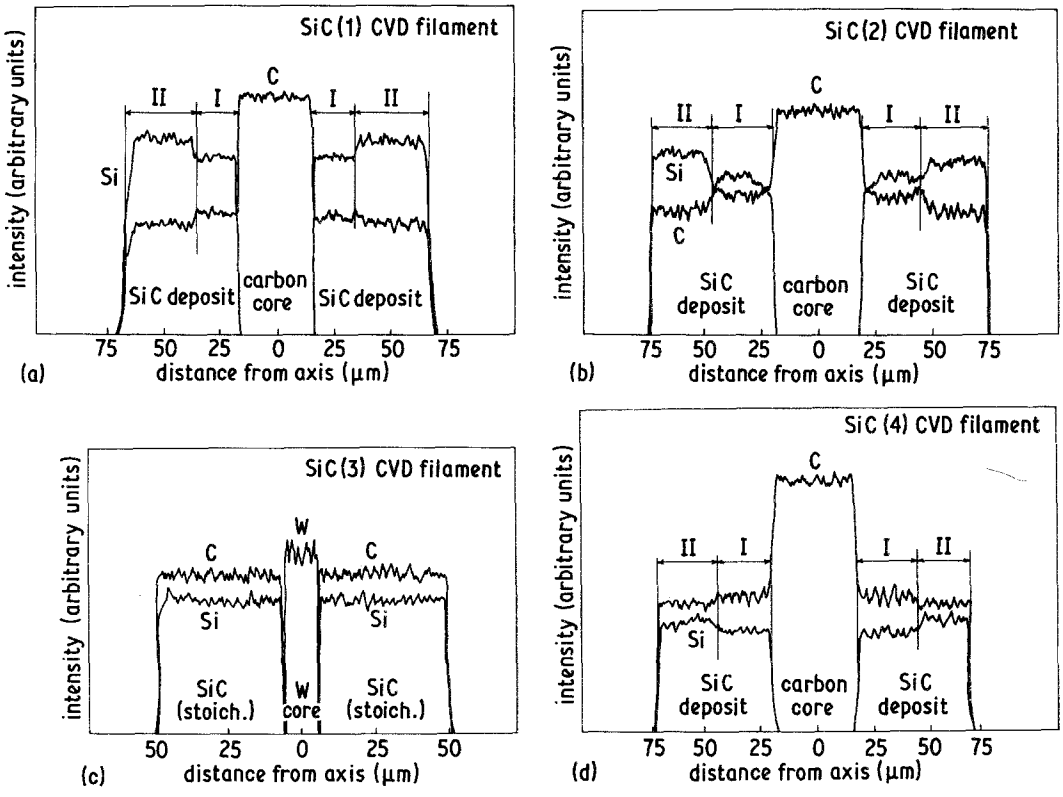

Figure 8 Auger radial profiles for silicon (Si_{LMM}), carbon (C_{KLL}) and tungsten (W_{MNN}) in SiC based CVD filaments.

and SiC(4)), but no attempt was made to identify the α-SiC polytype to which they could correspond. The occurrence of small amounts of α-SiC in β-SiC CVD deposits obtained at 1200 to 1400° C (i.e. far below the $\beta \rightarrow \alpha$ transition temperature), seems to be common and has been already reported by several authors [22, 29, 31].

One line ($d = 0.336$ to 0.340 nm) has been attributed to graphite (d_{002}). It is observed only for SiC(1) and SiC(2) filaments, i.e. for those

TABLE II Debye–Scherrer patterns of SiC based CVD filaments (The filaments were directly exposed to a X-ray source without grinding)

SiC(1)		SiC(2)		SiC(3)		SiC(4)	
3.4	25*	3.36*		–		–	
				2.7	25¶		
2.52	100†	2.50	100†	2.50	100†	2.51	100†
–		–		2.24	25§	–	
2.18	10†	2.16	10†	2.18	10†	2.17	10†
1.91	25‡	–		2.01	25‡	2.00	25‡
1.85	25	–		1.85	25‡	1.85	25‡
–		–		1.70	25‡	1.69	25‡
–		–		1.58	25§	–	
1.54	75†	1.53	75†	1.54	75†	1.53	75†
1.31	50†	1.31	50†	1.31	50†	1.32	50†
–		–		1.29	25§	–	
1.258	25†	1.254	25†	1.258	25†	1.255	25†

*graphite.
†cubic β-SiC.
‡hexagonal α-SiC.
§tungsten.
¶unidentified.

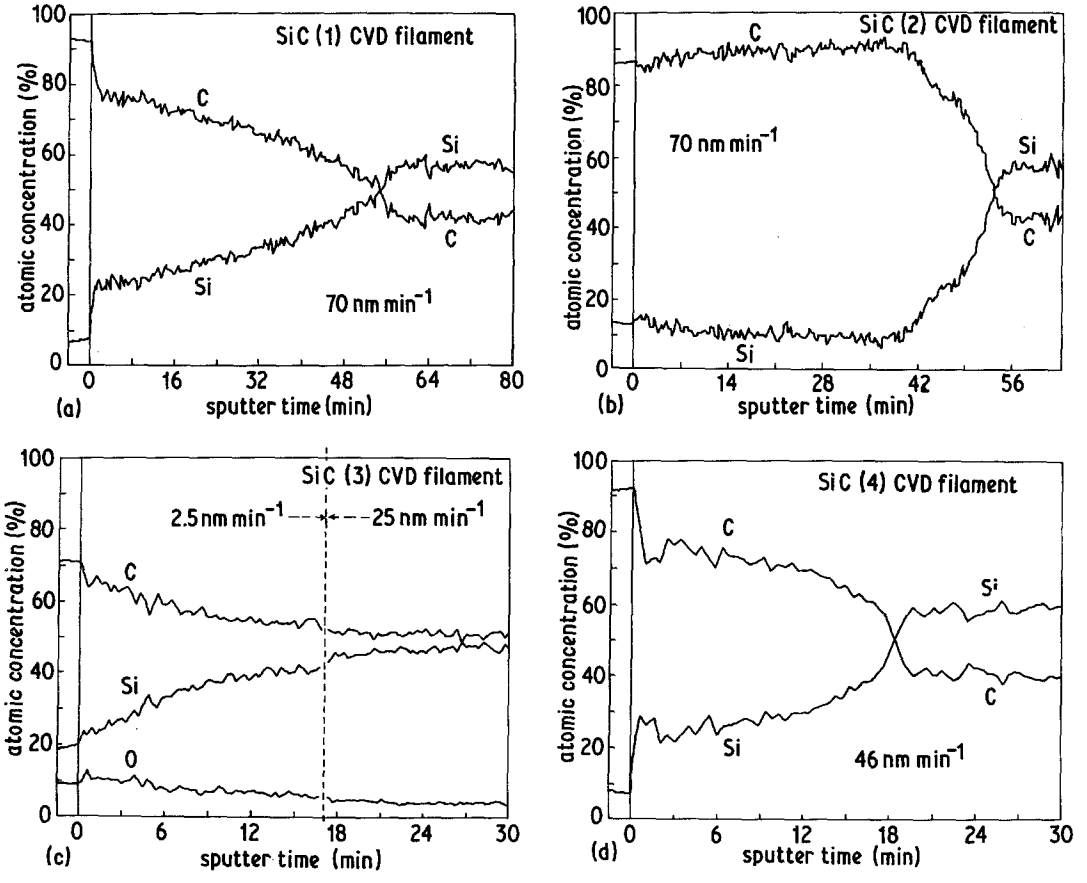

Figure 9 Auger depth profiles for silicon (Si_{LMM}), carbon (C_{KLL}) and oxygen (O_{KLL}) near the external surface of SiC-based CVD-filaments (the sputtering rate refers to tantalum oxide Ta_2O_5 used as a standard).

found by Auger microprobe analysis to have received a rather thick ($\simeq 4\,\mu m$) carbon-rich surface coating.

Finally, a few faint lines are noted in the Debye–Scherrer pattern of the SiC(3) filament. They have been assigned to the tungsten core.

No significant modifications in the Debye–Scherrer patterns were observed after annealing treatments (24 h) at 850° C under vacuum.

6. Raman microprobe (MOLE) analysis

Raman spectroscopy has been found to be a powerful tool to characterize poorly organized solids as well as their evolution towards well ordered materials. As an example, it has been successfully utilized for the analysis of the carbons resulting from the pyrolysis of liquid (or gaseous) precursors and for the study of their graphitization [33–35]. Since SiC-filaments are also obtained by pyrolysis of a gaseous mixture at medium temperature and contain pyrocarbon, as established above, it was thought that the Raman microprobe analysis could be used for a better understanding of the microstructure of SiC-based CVD filaments [21–36].

The Raman MOLE microanalyser (argon ion laser; 514.5 nm emission line) has been used with its maximum spatial resolution (about $1\,\mu m^2$) and with a spectral resolution of the order of $8\,cm^{-1}$. The spectra of the SiC-filaments were recorded from the polished sections of SiC–Ti composites already used in the X-ray and Auger microanalyses. They are given in Fig. 10.

The Raman spectra are characterized by two series of lines, more or less broad according to the ordering state of the material. The first series consists of two strong lines at 800 and $970\,cm^{-1}$ assigned, respectively, to the TO and LO Raman active modes expected for the cubic low temperature β-modification of SiC, superimposed on broad features centred at about 800 and $500\,cm^{-1}$ (which could be assigned to a disorganized form of SiC). The second series consists of two strong lines at 1600 and $1350\,cm^{-1}$ due to pyrocarbon. The

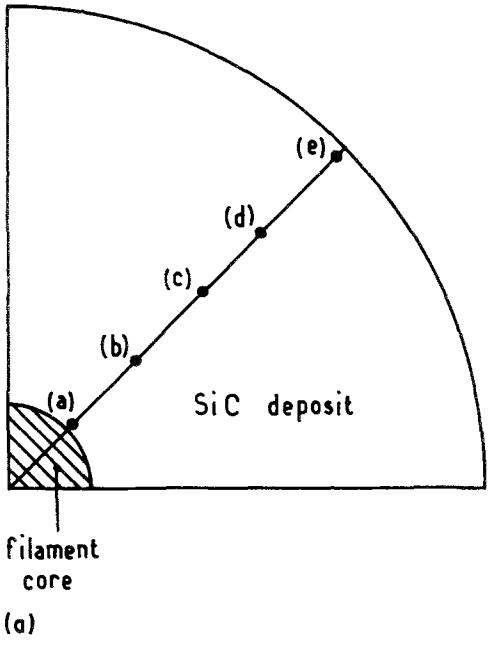

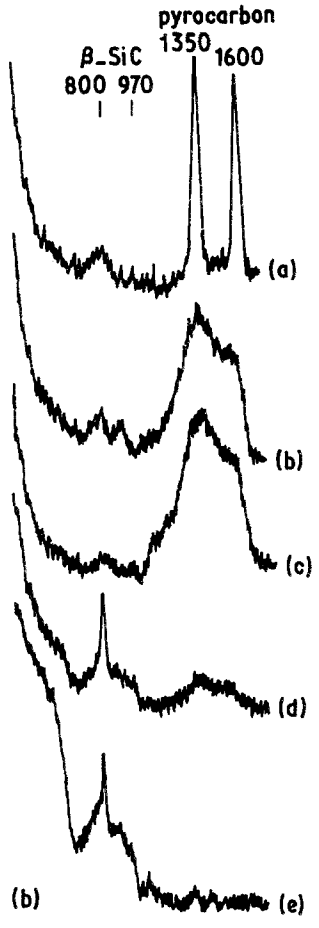

Figure 10 Raman spectra of SiC based CVD-filaments. The points in Fig. 10a represent (a) 5 μm from the core, (b) 1/4 SiC deposit, (c) 1/2 SiC deposit, (d) 3/4 deposit, and (e) near external surface. (b) Raman spectra of SiC(1) CVD filaments. (c) Raman spectra of SiC(2) CVD filaments. (d) Raman spectra of SiC(3) CVD filaments. (e) Raman spectra of SiC(4) CVD filaments.

presence of crystalline α-SiC could not be confirmed by Raman analysis probably because its proportion was too weak with respect to those of β and non crystalline SiC [33, 35, 36].

In the case of the tungsten core SiC(3) filament, only the lines assigned to SiC are observed, very sharp and strong near the core and becoming faint and broad when moving towards the filament surface (this feature probably being related to a decrease in the state of crystallization of SiC in the outer part of the filament).

The case of the carbon core filaments is more complex. However, the occurrence of two zones suggested, for the inner one, a mixture of SiC and carbon and, for the outer one, almost pure SiC, is confirmed. Within each zone, the state of crystallization of both components undergoes an evolution when moving towards the filament surface. As an example, in the inner part of SiC(1), carbon in the SiC+C mixture near the carbon core exhibits sharp and strong lines at 1600 and 1350 cm^{-1} characteristic of rather well organized graphitic planes. But it becomes less organized (and possibly amorphous) when moving apart, as supported by a wide broadening of these lines. On the other hand, SiC remains poorly crystallized within the whole inner part. In the outer part of the filament, the deposit contains less and less carbon (poorly crystallized) as moving towards the filament surface, but SiC has a somewhat better crystallization state. This is still more important in the case of the SiC(4) filament [35].

7. Scanning electron microscope analysis

Fig. 11 gives a SEM analysis of the fracture surface (tensile tests) of the SiC-based filaments that confirms the occurrence of two concentric deposits, tightly bound together and of different width, in the case of the carbon-core filaments. The fracture surfaces are smooth for SiC(1) and SiC(4) and irregular for SiC(2) and SiC(3). Finally, the carbon core wire seems to have received a thin coating (a few microns in thickness) before SiC-deposition, identified as pyrocarbon (see Auger and Raman analyses).

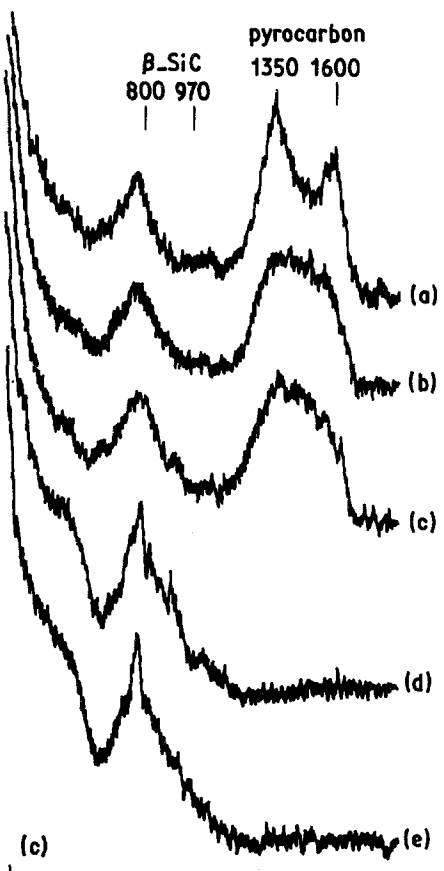

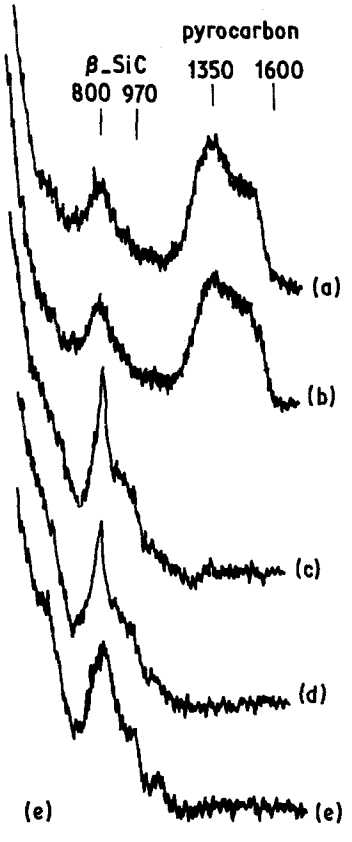

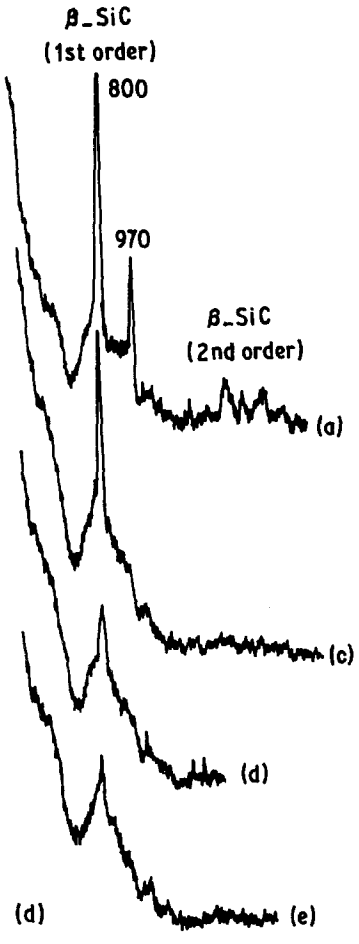

Figure 10 Continued.

8. Strength characterization of the filaments

The filament strength was measured at room temperature, with a tensile machine equipped with a 500 N load cell and pneumatic grips, at a crosshead speed of 1 mm min^{-1}. The gauge length of filament was cemented at each end in a paperholder card with an epoxy resin, as illustrated in Fig. 12. This simple device greatly facilitates the filament alignment along the tensile axis and reduces the occurrence of sliding and breaking within the grips (less than 1%). The paper holder was cut just before application of the load to the filament. Strength measurements were performed on each type of filament and, in a few cases, at different gauge lengths. An average of 50 filaments were tested in each case.

The distribution of the results are shown in Fig. 13. For a medium gauge length (40 mm), the three carbon-core 140 μm filaments appear to be

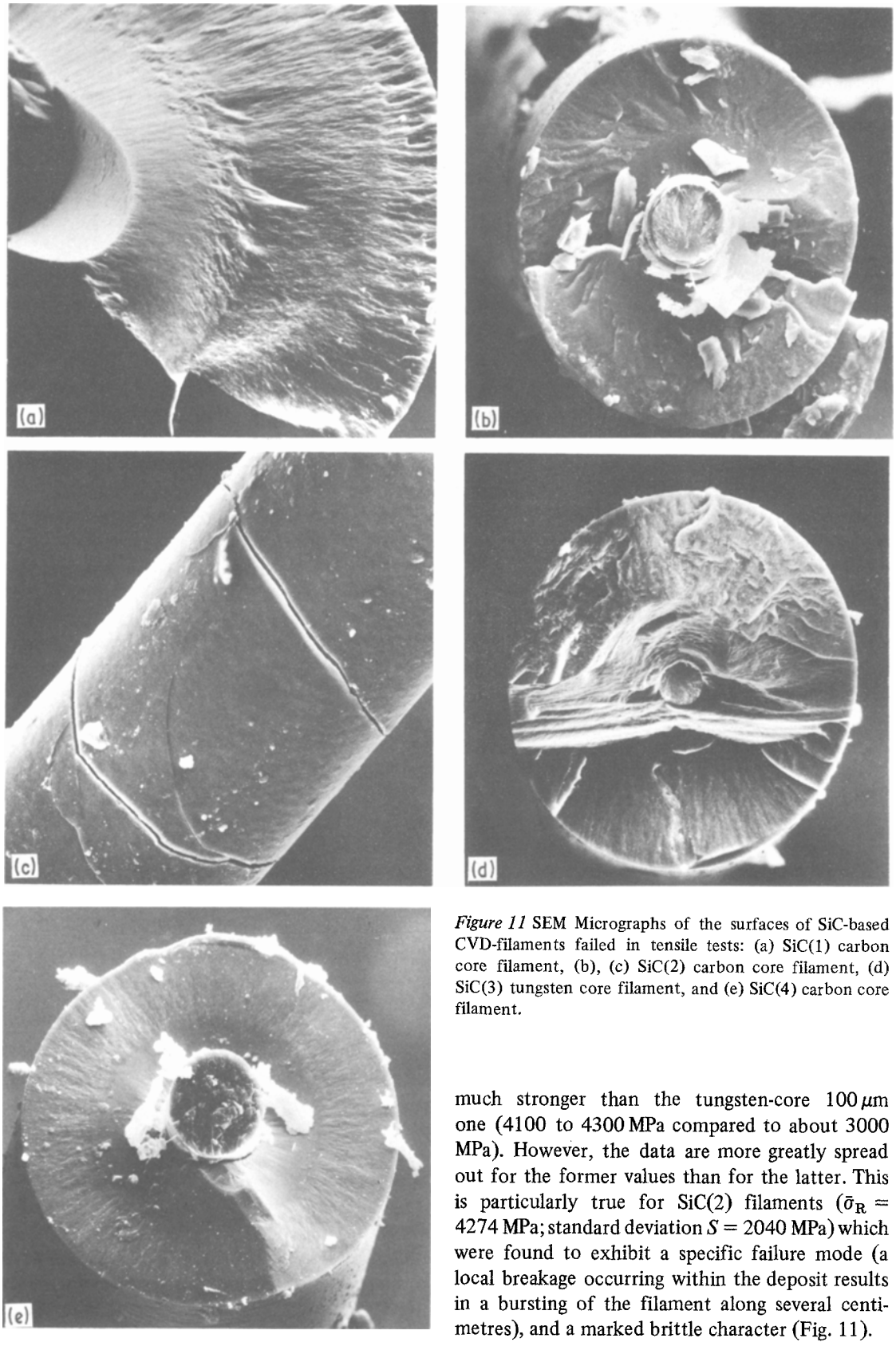

Figure 11 SEM Micrographs of the surfaces of SiC-based CVD-filaments failed in tensile tests: (a) SiC(1) carbon core filament, (b), (c) SiC(2) carbon core filament, (d) SiC(3) tungsten core filament, and (e) SiC(4) carbon core filament.

much stronger than the tungsten-core 100 μm one (4100 to 4300 MPa compared to about 3000 MPa). However, the data are more greatly spread out for the former values than for the latter. This is particularly true for SiC(2) filaments ($\bar{\sigma}_R$ = 4274 MPa; standard deviation S = 2040 MPa) which were found to exhibit a specific failure mode (a local breakage occurring within the deposit results in a bursting of the filament along several centimetres), and a marked brittle character (Fig. 11).

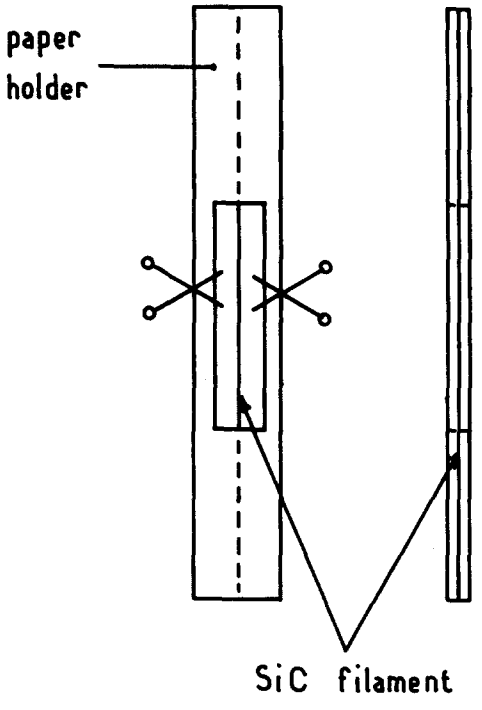

Figure 12 Filament sample holder used for tensile strength measurements.

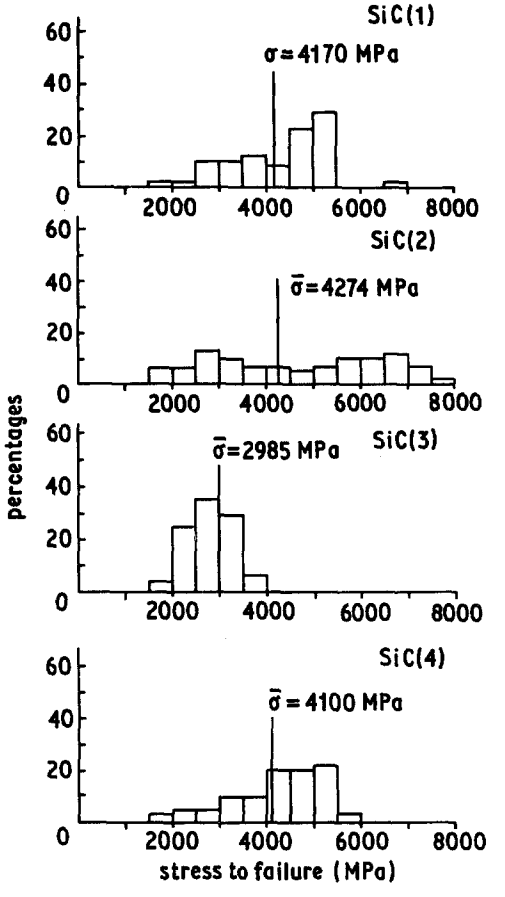

Figure 13 Tensile strength distribution for SiC based CVD-filaments (gauge length: 40 mm, ~ 50 filaments were tested at room temperature, in each case).

As expected from the brittleness of SiC-based CVD filaments, their mean strength is a function of the gauge length. As an example, increasing the gauge length from 20 to 60 mm decreases the mean strength from 4000 to 3400 MPa in the case of SiC(4) filaments (Fig. 14). These results corroborate those given by Cantagrel and Marchel [6] on tungsten-core filaments (very similar to SiC(3)), reporting that $\bar{\sigma}_R$ decreases when the gauge length increases from 4 to 100 mm and then remains almost constant when it further increases up to 300 mm.

Finally, the room temperature strength of SiC-based CVD filaments is not significantly modified after heat treatment, under vacuum during several hours at 850° C (the processing temperature of the SiC/Ti composites) as illustrated in Fig. 15.

9. Weibull treatment of the tensile test data

9.1. The Weibull distribution function

As illustrated above and already underlined by several investigators, SiC-based CVD-filaments are characterized by a variable strength which can be attributed to the existence of a statistical population of flaws. The statistical character of the filament strength is often analysed on the basis of the Weibull distribution function [37–41].

According to the Weibull statistics, the probability of survival P_s of a filament loaded at stress σ is a function of its volume and is given by the following empirical equation:

$$P_s = \exp\left|-V\left(\frac{\sigma-\sigma_u}{\sigma_0}\right)^m\right| \qquad (1)$$

where V is the volume of the filament, σ_u is the stress below which failure never occurs (usually assumed to be zero), σ_0 is the scale parameter, and m is the shape or flaw dispersion parameter. σ_0 and m are constant for a given material. The so-called Weibull modulus m is a measure of the strength dispersion or of the flaw spatial distribution in the filament. Assuming that $\sigma_u = 0$ and that the filament diameter is constant along the length L corresponding to the volume V, Equation 1 can be written as:

$$\ln \ln 1/P_s = m \ln \sigma + \text{constant} \qquad (2)$$

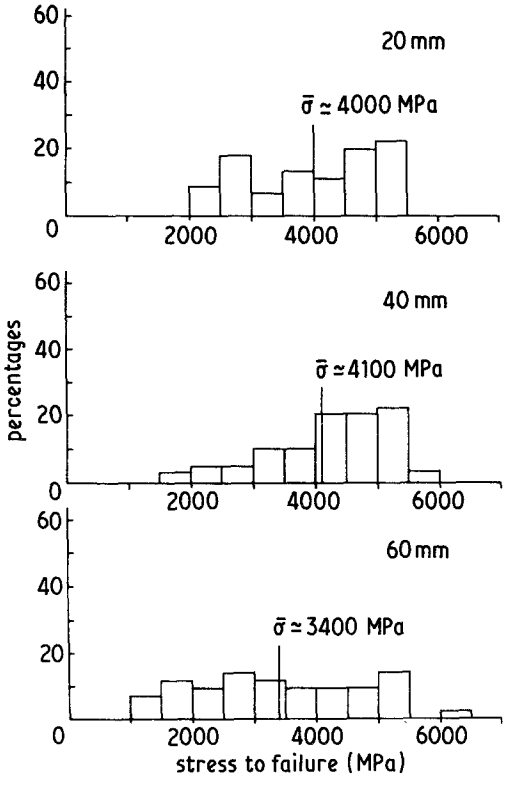

Figure 14 Tensile strength distribution for SiC(4) CVD-filaments at different gauge lengths (~ 50 filaments were tested at room temperature in each case).

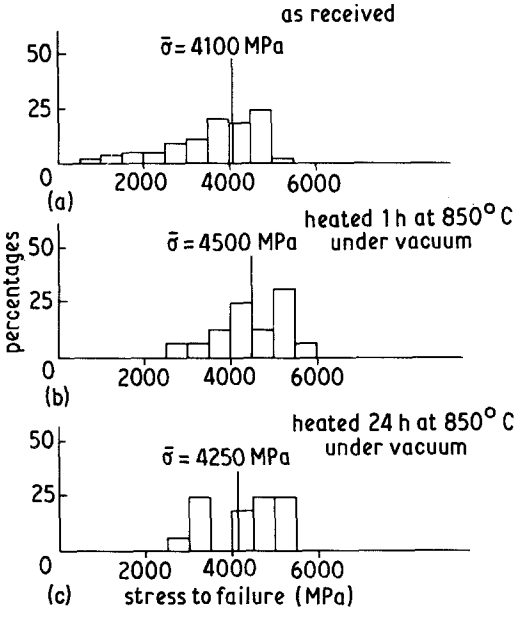

Figure 15 Tensile strength distribution for SiC(4) CVD-filaments (gauge length: 40 mm; ~ 50 filaments were tested at room temperature in each case).

which shows that the plot of ln ln $1/P_s$ as a function of ln σ, for a set of filaments having the same length, must be a straight line (if the filament strength does obey the Weibull equation). In such a case the slope is the Weibull modulus m.

Furthermore, the median strength of the filament $\sigma_{0.5}$ (corresponding to $P_s = 0.50$) is a function of its length L (if it can be regarded as of constant diameter) and is given by following equation:

$$\ln \sigma_{0.50} = -1/m \ln L + \text{constant} \qquad (3)$$

which shows that the plot of ln $\sigma_{0.50}$ against ln L must also be a straight line, with a slope equal to $-1/m$.

Finally, the coefficient of variation C_V, which is defined in the case of tensile tests by:

$$C_V = \frac{S}{\bar{\sigma}},$$

where $\bar{\sigma}$ is the mean tensile strength and S the corresponding standard deviation, is found to depend only on m, if $\sigma_u = 0$

$$C_V = \frac{S}{\bar{\sigma}} = \left[\frac{\Gamma\left(1 + \frac{2}{m}\right)}{\Gamma\left(1 + \frac{1}{m}\right)^2} - 1 \right]^{1/2} \qquad (4)$$

where $\Gamma(x) = \int_0^\infty e^{-x} x^{n-1}\, dx$ is the tabulated gamma function. A good approximation of C_V, mentioned by Street and Ferte [37] is:

$$C_V \simeq m^{-0.94}$$

9.2. ln ln $1/P_s$ against ln σ Weibull plots

The ln ln $1/P_s$ against ln σ Weibull plots are given in Figs. 16a to c for the various SiC based CVD-filaments. It appears that:

1. The plot is indeed almost a straight line over the full σ range for SiC(3) tungsten-core filaments (Fig. 16a). The Weibull modulus m, determined from the slope (Equation 2) is rather high and equal to 7 to 8 (Table III).

2. The plots are almost identical for SiC(1) and SiC(4) carbon-core filaments (Fig. 16b). They can still be regarded, at least in first approximation, as straight lines. However the corresponding Weibull modulus, $m = 4$ to 5, is lower than that found for SiC(3) (Table III).

3. Finally the strength distribution data are much more spread out along the σ axis, in the case of SiC(2) carbon-core filaments. In this case, fitt-

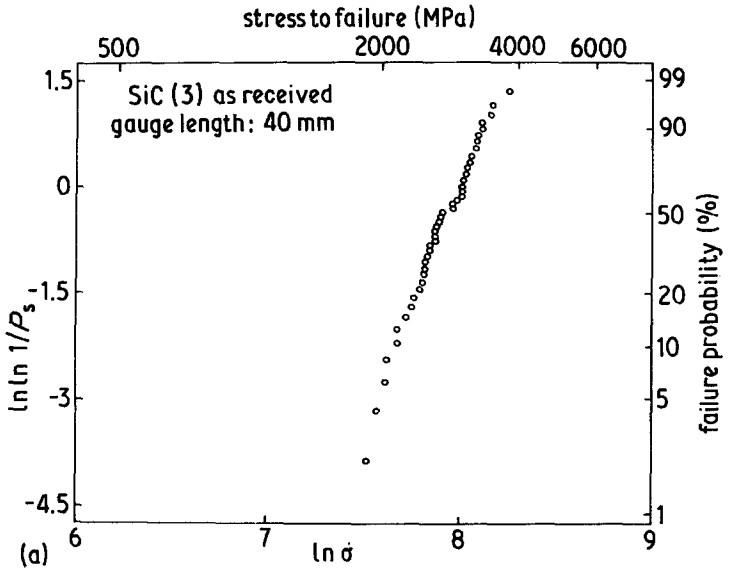

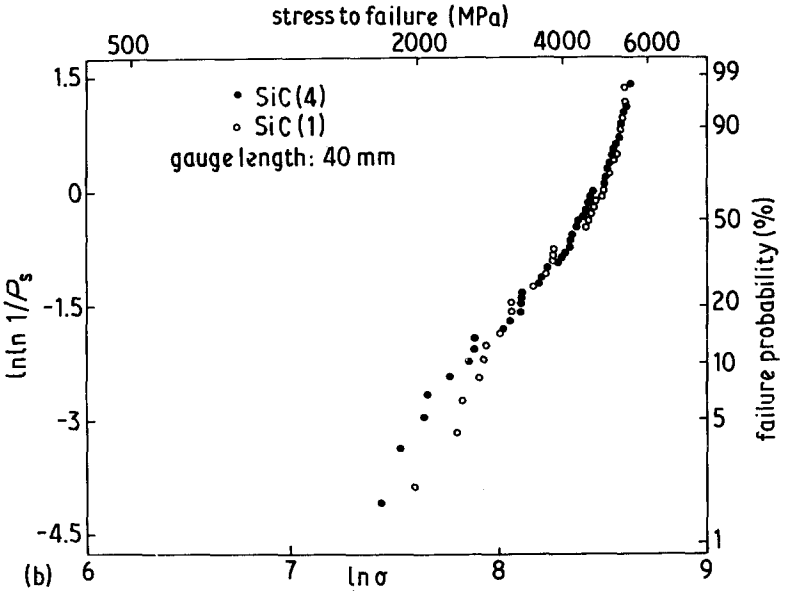

Figure 16 ln ln $1/P_s$ against ln σ Weibull plots for SiC based CVD-filaments (a) SiC(3) tungsten core filaments, (b) SiC(1) and SiC(4) carbon core filaments, and (c) SiC(2), SiC(4) (carbon core) and SiC(3) (tungsten core) filaments.

TABLE III Weibull modulus m and scale parameter σ_0 for the SiC based CVD filaments (carbon or tungsten core)

Filaments	$\bar{\sigma}$ (MPa)	S (MPa)	$C_v = \frac{S}{\bar{\sigma}}$	m (meas.)*	m from C_v†	σ_0 (MPa)*
SiC (1) carbon core	4170	1200	0.29	5.2	3.7	9300
SiC (2) carbon core	4274	2040	0.48	2.2	2.2	25800
SiC (3) tungsten core	2985	660	0.22	7.9	5.0	5060
SiC (4) carbon core	4100	1050	0.25	4.2	4.4	10900

*Derived from the ln ln $1/P_s$ against ln σ mean straight lines given in Fig. 16.
†Calculated from $C_v \simeq m^{-0.94}$.

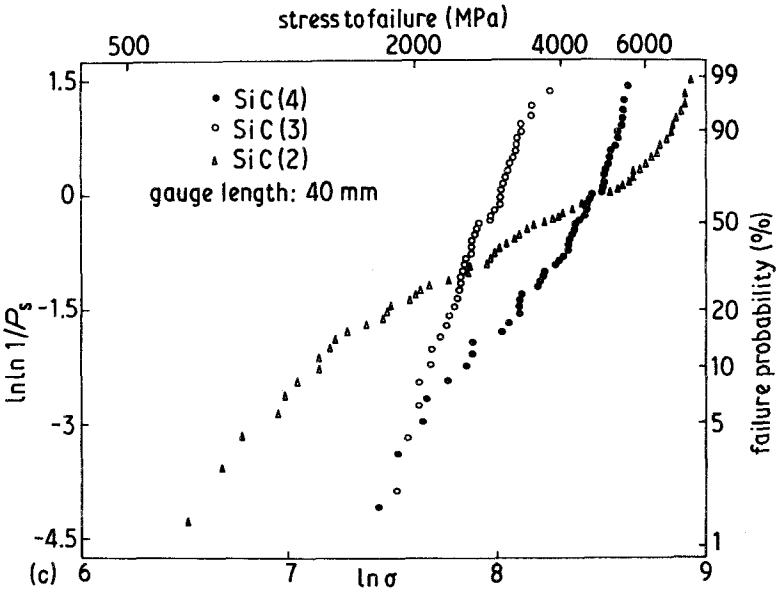

Figure 16 Continued.

ing the data with a single straight line is only a very rough approximation. The corresponding Weibull modulus is still lower and equal to about 2. The data could be better accounted for on the basis of three straight lines characterized by different Weibull moduli: $\simeq 5$ at lower stress, $\simeq 2$ at medium stress and $\simeq 4$ at higher stress. This result seems to support the presence of a complex (or multimodal) flaw distribution.

9.3. ln $\sigma_{0.5}$ against ln L Weibull plots

The variation of the median strength $\sigma_{0.5}$ as a function of the gauge length L has been studied in the case of SiC(4) filaments. The ln $\sigma_{0.5}$ against ln L plot is given in Fig. 17.

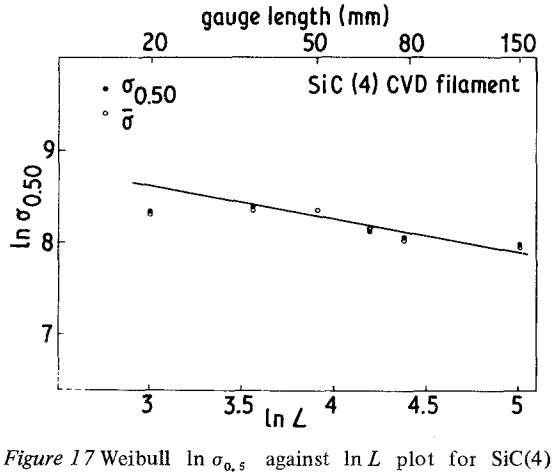

Figure 17 Weibull ln $\sigma_{0.5}$ against ln L plot for SiC(4) filaments.

The data are well fitted with a single straight line except for the smallest gauge length. The corresponding Weibull modulus m, derived from the slope (Equation 3), is equal to about 3, a value somewhat lower than that previously found ($\simeq 4$).

Finally, it appears that $\sigma_{0.5}$ and $\bar{\sigma}$ are almost identical.

9.4. Weibull modulus derived from the coefficient of variation

Assuming that the strength data obey the Weibull equation, m can be calculated from the coefficient of variation C_v, according to Equation 5. The results are given in Table III.

10. General discussion

The results of the chemical analyses and of the tensile tests reported above show that tungsten core SiC-filaments on one hand and carbon core SiC-filaments on the other hand are obviously rather different from both the structure and the strength standpoints. The former, made of a homogeneous stoichiometric SiC deposit, are significantly weaker ($\bar{\sigma}_R \simeq 3000$ MPa) than the latter made of a complex SiC/C deposit characterized by a much higher strength ($\bar{\sigma}_R \simeq 4100$ MPa).

The homogeneous chemical composition (nearly stoichiometric SiC within the whole deposit) found for SiC(3) agrees well with what could be expected from the reported CVD-conditions (pyrolysis of a CH_3SiCl_3–H_2 mixture at 1200 to

1300° C in a single stage hot wall deposition chamber) [6]. Although the $\alpha = [H_2]/[MTS]$ value was not mentioned, it must be close to the α_i limit (Fig. 2). The different types of defects that may control failure of tungsten core SiC-filaments have already been analysed by several investigators. It is usually accepted that failure is mainly initiated by: surface defects at low stresses (below $\simeq$ 2200 MPa) and by defects located either within the tungsten core or near the SiC-deposit/tungsten substrate interface at high stresses (above $\simeq$ 3100 MPa). At medium stresses (i.e. $2200 < \sigma_R < 3100$ MPa) both types of defects are active [9, 16, 42]. The bimodal character of tungsten core SiC-filament failures has been also underlined by Gruber [40] (his tensile test data were accounted for on the basis of two Weibull straight lines, with $m = 16.3$ at low stress and $m = 6.7$ at high stresses). Figs. 13 and 16a show that the failure stress found for SiC(3) filaments does fall within this stress range. Furthermore, the rather high value of the Weibull modulus ($m \simeq 8$) suggests that the flaws are present in large number and evenly distributed through the material (explaining thus that there is little scattering in the individual failure strengths) [39]. The occurrence of surface defects could be related to degradation due to handling (the SiC-filament surface is thought to be in tension whereas that of boron filament is in compression and therefore less sensitive to degradation [16] and to the fact that no surface coating was applied on SiC(3) filaments (as shown by Auger analysis). Failure that occurs near the SiC deposit/tungsten core interface could be explained both by defects resulting from some chemical reaction between SiC and tungsten (such a reaction, even if it is less extended than for boron filaments, seems actually to occur, as shown by Random *et al.* [42] for example) or/and by recrystallization of SiC (favoured by the vicinity of the hot tungsten wire) as shown by Raman analysis (Fig. 10). As a matter of fact, SiC(3) is the only filament in which SiC was found well crystallized, particularly near the metal core [42].

It seems likely that the carbon core SiC-filaments have been developed to minimize the number of surface defects (by applying a suitable surface-coating) and of defects located near the core/deposit interface (by replacing the reactive tungsten substrate by a material, i.e. carbon, having a better chemical compatibility with SiC). The complex internal structures observed for SiC(1), SiC(2) and SiC(4) carbon core filaments illustrate part of the efforts made by the producer during the last years to optimize their strength and chemical compatibility with metal matrices [7–9, 16–18].

The increase in strength seems to be related to: (i) the excellent compatibility between the carbon core and the SiC-deposit, (ii) the occurrence of two concentric SiC-based deposits of different compositions, (iii) the rather poor state of crystallization of SiC (see Fig. 10), and (iv) the external thin coating of pyrocarbon (or of carbon rich deposit). In absence of any significant chemical reaction at the core/deposit interface the stress concentrators that strongly lowered the strength of the tungsten core filaments do not arise. In the same manner, coating the filament with a thin layer of pyrocarbon is reported to be an efficient way to suppress the surface sensitivity of SiC-filaments to abrasion (e.g. that due to handling) [9]. Although it is known that the properties of SiC are sensitive to impurities such as free carbon, it is not clear why the best results seem to be obtained when the deposit is made of an inner layer of carbon-rich SiC surrounded by an outer layer of almost stoichiometric SiC, both having approximately the same thickness, as reported by Debolt and Henze [17]. The interest of the CVD-process lies in the fact that SiC–C mixtures, ranging from almost pure SiC to pure carbon, can be deposited in the same reactor by modifying the gas phase composition, as illustrated in Fig. 1–6. Thus, according to Debolt and Henze, carbon-rich (plateau I) is deposited from a mixture of chlorosilanes (mainly $(CH_3)_2SiCl_2$ and CH_3SiHCl_2) hydrogen and propane in the ratios 6/2/1, while stoichiometric SiC (plateau II) is obtained from an hydrogen-rich mixture of chlorosilanes and hydrogen (1/2 ratio). Finally, an addition of argon favours the formation of carbon (see Fig. 5) and increases locally the deposition temperature (argon has a lower thermal conductivity than hydrogen).

Coating SiC filaments with a thin layer of pyrocarbon, if it does reduce their sensitivity to surface abrasion (e.g. that due to handling) also modifies their chemical reactivity towards metal matrices. Moreover, it is known that carbon is not spontaneously wetted by liquid metals such as aluminum alloys and reacts with them more rapidly than silicon carbide. This is probably the reason why a new carbon core SiC filament (referred to as SCS) has been recently developed

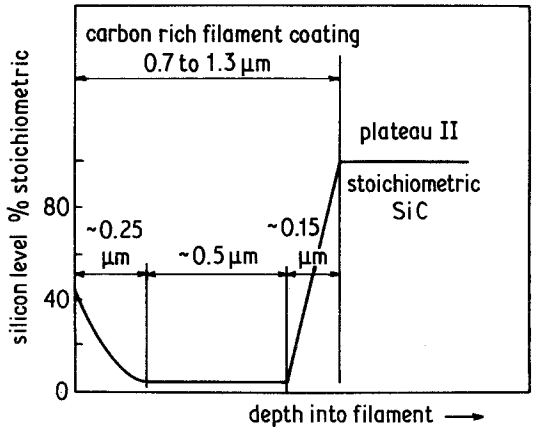

Figure 18 SiC/C external coating in SiC-based CVD-filaments (SCS type) according to Debolt *et al.* [18].

by AVCO [18]. It has a SiC/C coating (0.7 to 1.3 μm thick) characterized by a composition gradient, as shown in Fig. 18. This coating is made of nearly pure pyrocarbon close to the inner SiC deposit (plateau II) surrounded by a thin layer of a SiC/C mixture in which the amount of SiC progressively increases as the external surface of the filament is reached [18]. The Auger depth profiles given in Fig. 9 show that none of the analysed carbon core filaments belongs to this type. According to Nutt *et al.* [44] the SCS filament has an improved chemical compatibility with metal matrices.

The results of the tensile tests clearly show that annealing the filaments under vacuum at 850° C (i.e. under conditions similar to those used for the synthesis of the SiC/Ti composites) does not lower their strength (a slight increase is even usually observed, as shown in Fig. 15). This result is in opposition with that reported by House [43] according to which a 50% strength loss may occur after only one hour of annealing under high vacuum at 875° C. The only difference in the annealing procedures lies in the fact that the samples were sealed in silica glass tubes in present work and apparently directly heated in a vacuum furnace in the House [43] experiments.

In conclusion, our analyses have shown that the tungsten core SiC(3) filaments are made of a homogeneous deposit of nearly stoichiometric SiC with no surface coating. Their rather low mean strength is probably related to two types of defects located at their surface and near the core/deposit interface. The carbon core filaments are much stronger and all of them have received a surface coating which is of almost pure pyrocarbon for SiC(2) and of a carbon-rich SiC+C mixture for SiC(1) and SiC(4). The failures of all the carbon core filaments appear to have a multimodal character, SiC(2) having the highest brittleness, the largest strength distribution ($m \sim 2$) and thus requiring the most handling care.

It will be considered in the following articles that SiC(1) and SiC(4) filaments are almost identical. The above analyses also suggest that the chemical reactivity of the filaments towards titanium mignt logically increase from SiC(3) (almost stoichiometric SiC) to SiC(2) (almost pure carbon at the external surface) as far as the external coating is not totally consumed, SiC(1) or SiC(4) being intermediate cases.

Acknowledgements

The authors wish to thank AVCO, SEP and SNPE for the filament supply. This work has been partly supported by a CNRS-ATP contract.

References

1. A. G. METCALFE, *J. Compos. Mater.* **1** (1967) 356.
2. M. J. KLEIN and A. G. METCALFE, Effect of Interfaces in Metal-matrix Composites on Mechanical Properties, AFML Technical Report 71-189 (1971).
3. J. A. SNIDE, Compatibility of Vapor Deposited B, SiC and TiB_2 Filaments with Several Titanium Matrices, AFML, Technical Report 67-354 (1968).
4. M. J. KLEIN, M. L. REID and A. G. METCALFE, Compatibility Studies for Viable Titanium Matrix Composites, AFML Technical Report 69-242 (1969).
5. S. OCHIAI and Y. MURAKAMI, *J. Mater. Sci.* **14** (1979) 831.
6. M. CANTAGREL and M. MARCHAL, *Rev. Int. Hautes Temp. Réfract.* **9** (1972) 93.
7. E. FITZER, D. KEHR, D. MORIN and M. SAHEBKAR, Proceedings of the Vth International Conference CVD, September 1979 edited by J. M. Blocher, H. E. Hintermann and L. H. Hall (The Electrochem. Soc., Princeton, 1975) pp. 589–599.
8. H. E. DEBOLT, V. J. KRUKONIS and F. E. WAWNER, Proceedings of the International Conference on SiC, Miami, September 1973, edited by R. C. Marshall, J. W. Faust and C. E. Ryan (University of South Carolina Press, Columbia, South Carolina, USA, 1974) pp. 168–175.
9. *Idem*, Proceedings of SAMPE no. 19, Azusay, California, 1974, pp. 328–339.
10. S. YAJIMA, K. OKAMURA, J. HAYASHI and M. OMORI, *J. Amer. Ceram. Soc.* **59** (1976) 324.
11. S. YAJIMA, H. KAYANO, K. OKAMURA, M. OMORI, J. HAYASHI, T. MATSUZAWA and K. AKUTZU, *Amer. Ceram. Soc. Bull.* **55** (1976) 12, 1065.

12. E. RUDY and St. WINDISCH, Ternary Phase Equilibria in Transition Metal Boron-Carbon-Silicon Systems, AFML Technical Report 65-2 (1966).
13. R. PAILLER, Thesis no. 616, University of Bordeaux-I (1979).
14. R. PAILLER, M. LAHAYE, J. THEBAULT and R. NASLAIN, Proceedings of the International Conference on "Failure Modes and Processing of Composites IV", Chicago, October 1977, edited by J. A. Cornie and F. W. Crossman (TSM-AIME, New York, 1979) pp. 265–284.
15. R. PAILLER, P. MARTINEAU, M. LAHAYE et R. NASLAIN, *Rev. Chimie Minérale* **18** (1981) 520.
16. R. L. CRANE and V. J. KRUKONIS, *Ceram. Bull.* **54/2** (1975) 184.
17. H. E. DEBOLT and T. W. HENZE, US Patent 4068 037, January 10 (1978).
18. H. E. DEBOLT, R. J. SUPLINSKAS, J. A. CORNIE, T. W. HENZE and W. HAUZE, US Patent 4340 636, July 20 (1982).
19. F. CHRISTIN, R. NASLAIN and C. BERNARD, Proceedings of the 7th International Conference on CVD, Los Angeles, October 1979, edited by T. O. Sedwick and H. Lydtin (The Electrochem. Soc., Princeton, 1979) pp. 499–514.
20. F. CHRISTIN, Thesis no. 641, University of Bordeaux-I (1979).
21. C. MALLET, Thesis no. 1811, University of Bordeaux-I (1982).
22. J. CHIN, P. K. GANTZEL and R. G. HUDSON, *Thin Solid Films* **40** (1977) 57.
23. J. CHIN and T. OHKAWA, *Nuclear Technol.* **32** (1977) 115.
24. P. POPPER and I. MOHYUDDIN, in "Special Ceramics", edited by P. Popper (Academic Press, London, New York, 1965) pp. 45–59.
25. M. J. CHAPPELL and R. S. MILLMAN, *J. Mater. Sci.* **9** (1974) 1933.
26. P. POPPER and R. L. RILEY, *Proc. British Ceram. Soc.* **7** (1967) 99.
27. T. D. GULDEN, *J. Amer. Ceram. Soc.* **51** (1968) 424.
28. J. I. FEDERER, *Thin Solid Films* **40** (1977) 89.
29. J. R. WEISS and R. J. DIEFENDORF, *J. Electrochem. Soc.* **3** (1973) 585.
30. E. L. KERN, D. W. HAMILL and K. A. JACOBSON, Proceedings of the 14th SAMPE National Symposium on "Advanced Techniques for Material Investigation and Fabrication" (Cocoa Beach Fla, 1968, II-2B-3.
31. J. E. SPRUIELL, ORNL-4326, Oak Ridge National Laboratory, Tenn., USA, (December 1968).
32. J. SCHLICHTING, *Powder Metallurgy Intern.* **12** (1980) 141, 196.
33. M. COUZI and F. CRUEGE, *L'actualité chimique* (April 1980) 62.
34. A. MARCHAND, P. LESPADE and M. COUZI, Proceedings of the 15th International Conference on Carbon, Philadelphia, August 1981 (Pennsylvania University, Pennsylvania, 1981) pp. 282–284.
35. P. LESPADE, Thesis no. 325, University of Bordeaux-I (1982).
36. M. COUZI, F. CRUEGE, P. MARTINEAU, C. MALLET and R. PAILLER, Proceedings of the 17th Annual Meeting of the Microbeam Analysis Society, Phoenix, 1983 (to be published).
37. K. N. STREET and J. P. FERTE, Proceedings of the First International Conference Composite Materials (ICCM-1) Geneva, Boston, April, 1975, Vol. 1, edited by E. Scala, E. Anderson, I. Toth and B. R. Noton, pp. 137–163.
38. R. G. BARROWS, Failure Modes in Composites IV, Chicago, 1977, edited by J. A. Cornie, F. W. Crossman, (The Metallurgical Society of AIME, New York, 1979) pp. 45–72.
39. J. W. HITCHON and D. C. PHILLIPS, *Fiber Sci. Technol.* **12** (1979) 217.
40. P. E. GRUBER, Proceedings of the 2nd International Conference Mechanical Behavior of Materials (ASM, Metal Park Ohio, 1976) pp. 1330–1334.
41. G. SIMON and A. R. BUNSELL, Proceedings of the 3rd Journées Nationales sur les Composites (JNC-3), Paris, September 1982 (AMAC, Paris, 1982) pp. 195–206.
42. J. L. RANDON, G. SLAMA and A. VIGNES, Proceedings of the International Conference on SiC, Miami, September 1973, edited by R. C. Marshall, J. W. Faust and C. E. Ryan (University of South Carolina Press, Columbia, South Carolina, USA, 1974) pp. 386–393.
43. L. J. HOUSE, Thesis, The G. Washington University, District of Columbia, May (1979).
44. F. E. WAWNER, A. Y. TENG and S. R. NUTT, *Sampe Quaterly* **14/3** (1983) 39.

Received 6 September
and accepted 22 September 1983